

Elasto-Plastic Analysis of the Double Sheet Pile Wall Structure*

Kouichi OHORI**

Yoshihiro SHOJI**

Hiroshi UEDA**

Michihiko HARA***

Yutaka KAWAI***

Keisuke SHIOTA***

An elasto-plastic analysis was performed to investigate the characteristics of a double sheet pile wall structure. The analytical method is expanded from Sawaguchi's elastic theory to consider not only the interaction between sheet piles, tie rod, and filling sand but also footing ground.

The comparison between the theoretical predictions and experimental results has shown that the calculated values agree well with the experimental data concerning horizontal displacement of the wall top and with the bending moment distribution of sheet piles under distributed lateral load. As a result, it is clear that this method is useful in designing double sheet pile wall structures.

1 Introduction

The double sheet pile wall structure refers to a structure consisting of two rows of steel sheet piles with tops connected with tie-rods and spacings filled with sand so as to make up a wall. While this structure has merits of reduced space requirements, excellent water cutoff capability and good workability as a revetment structure, its design standards have not yet been established, because of its complicated mechanical behavior and also its former use mainly as a temporary structure. For this reason, the sectional factors are today determined by simulating design conditions for sheet pile walls¹⁾ or cellular cofferdams¹⁻³⁾. In fact, in order to utilize the merits of the double sheet pile mentioned above and find some reliable structure and form that can be used for permanent structures such as large-sized quaywall and revetment for storing industrial wastes, demand has for sometime been felt for an establishment of a specific design method.

Studies on the mechanical behavior of the double sheet pile wall structure involve plastic analysis by Mazurkiewicz⁴⁾, elastic analysis by Sawaguchi^{5,6)},

elastic analysis through the finite element method by Hirajima et al.⁷⁾, photoelastic analysis by Burki et al.⁸⁾, vibration tests by Arai, Takahashi, et al.^{9,10)}, and model experiments by Sawaguchi et al.¹¹⁾. Though these studies have clarified the behavior of this structure to some extent, it is not yet achievable to predict accurately important items for the practical design such as wall deformation under external load and bending moment of sheet pile.

For this reason, the authors adopted the fundamental equations of Sawaguchi⁶⁾ who considered the double sheet pile wall structure as a composite structure comprising sheet piles, tie-rods, filling sand and foundation ground, and derived general solutions that took into strict consideration the compressive deformation of filling sand and the passive resistance of ground which had previously been neglected or approximated. At the same time, they carried out the numeric calculation including the elasto-plastic behaviors of filling sand and ground, so as to represent the behavior of the double sheet pile wall structure quantitatively. The calculated values agreed relatively well with the measured values obtained in the experiment with small¹²⁾ and large-sized¹³⁾ models, demonstrating that the present calculation was effective for solving various design problems.

* Originally published in *Kawasaki Steel Giho*, 15(1983) 3, pp. 218-225

** Ministry of Transportation

*** Engineering Division

2 Derivation of Equations for Deformation of Structure Based on the Theory of Elasticity

2.1 General Solutions for Deflection of Structure

Like Sawaguchi⁶⁾, let us consider the equilibrium among horizontal forces acting upon a cross section per unit depth of the structure at a certain level, as shown in Fig. 1.

If stresses acting upon filling sand from sheet piles 1 and 2 are denoted by σ_1 and σ_2 , respectively, they are related to shearing force of filling sand S in the y -direction, as follows:

$$\sigma_1 - \sigma_2 = -\frac{dS}{dx} \quad \dots\dots\dots(1)$$

where x is perpendicular coordinate. If it is assumed that filling sand is a homogeneous elastic body with Young's modulus E_s and shear modulus G , S is represented in terms of average shear distortion of filling sand as below.

$$S = \frac{BG}{2} \left(\frac{dy_1}{dx} + \frac{dy_2}{dx} \right) \quad \dots\dots\dots(2)$$

y_1 and y_2 : Deflections of sheet piles 1 and 2, respectively,
 B : Wall breadth

From equations (1) and (2), the following equation for shear deflection is obtained:

$$\sigma_1 - \sigma_2 = -\frac{BG}{2} \left(\frac{d^2y_1}{dx^2} + \frac{d^2y_2}{dx^2} \right) \quad \dots\dots\dots(3)$$

and the equation for compressive deformation of filling sand is as follows.

$$\frac{\sigma_1 + \sigma_2}{2} = \frac{E_s}{B} (y_1 - y_2) \quad \dots\dots\dots(4)$$

On the other hand, if it is assumed that flexural rigidity EI for two rows of sheet piles are identical, the fundamental equations for sheet pile flexure are given by eq. (5).

$$\left. \begin{aligned} EI \frac{d^4y_1}{dx^4} &= -\sigma_1 + p_1 \\ EI \frac{d^4y_2}{dx^4} &= \sigma_2 + p_2 \end{aligned} \right\} \quad \dots\dots\dots(5)$$

p_1 and p_2 : External lateral force per unit area for sheet piles 1 and 2, respectively.

From eqs. (3), (4) and (5), two fundamental equations to describe the behavior of this structure can be derived as follows.

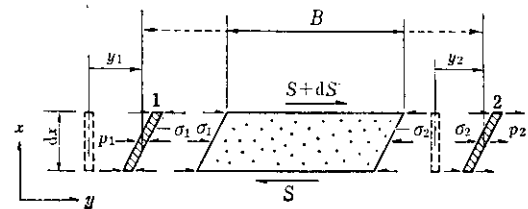


Fig. 1 Horizontal forces acting on a part of structure

$$EI \frac{d^4}{dx^4} (y_1 + y_2) = \frac{BG}{2} \frac{d^2}{dx^2} \cdot (y_1 + y_2) + p_1 + p_2 \quad \dots\dots\dots(6)$$

$$EI \frac{d^4}{dx^4} (y_1 - y_2) = -\frac{2E_s}{B} \cdot (y_1 - y_2) + p_1 - p_2 \quad \dots\dots\dots(7)$$

As for the external horizontal force acting upon the structure, head-concentrated load based upon wave force and impact force exerted by approaching ship, or load of triangular or trapezoidal distribution due to hydraulic pressure and back-filling earth pressure in case of cofferdam or revetment application were considered. Moreover, it is assumed that the penetrating segments of two-rows sheet piles are subjected to the passive resistance of ground in proportion to deflection. (See Fig. 2)

If deflections of sheet piles 1 and 2 within the ground are denoted by Y_1 and Y_2 , respectively, eqs. (6) and (7) are expressed as follows.

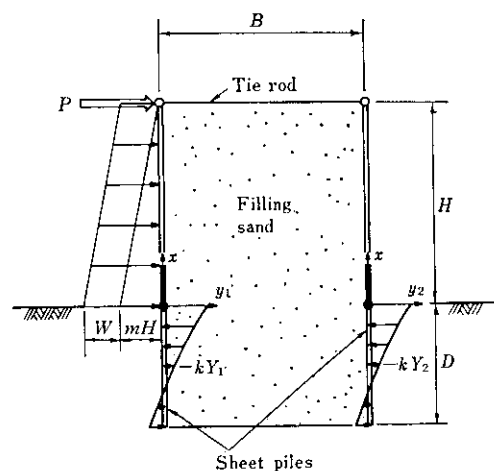


Fig. 2 Schematic model of structure

(1) Below ground ($x \leq 0$)

$$EI \frac{d^4}{dx^4}(Y_1 + Y_2) = \frac{BG}{2} \frac{d^2}{dx^2} \cdot (Y_1 + Y_2) - k(Y_1 + Y_2) \dots \dots \dots (8)$$

$$EI \frac{d^4}{dx^4}(Y_1 - Y_2) = -\left(\frac{2E_s + kB}{B}\right) \cdot (Y_1 - Y_2) \dots \dots \dots (9)$$

k : Coefficient of horizontal subgrade reaction

(2) Above ground ($x \geq 0$)

$$EI \frac{d^4}{dx^4}(y_1 + y_2) = \frac{BG}{2} \frac{d^2}{dx^2} \cdot (y_1 + y_2) + m(H - x) + w \dots \dots \dots (10)$$

$$EI \frac{d^4}{dx^4}(y_1 - y_2) = -\frac{2E_s}{B} \cdot (y_1 - y_2) + m(H - x) + w \dots \dots \dots (11)$$

H : Wall height,

m and w : Coefficients representing load distribution

General solutions for these differential equations are as given below:

(1) Below ground ($x \leq 0$)

From eq. (8),

(a) When $(BG)^2 > 16kEI$,

$$\left. \begin{aligned} Y_1 + Y_2 &= C_1 e^{\mu_1 x} + C_2 e^{\mu_2 x} \\ &+ C_3 e^{-\mu_1 x} + C_4 e^{-\mu_2 x} \\ \mu_1 &= \sqrt{\frac{BG + \sqrt{(BG)^2 - 16kEI}}{4EI}} \\ \mu_2 &= \sqrt{\frac{BG - \sqrt{(BG)^2 - 16kEI}}{4EI}} \end{aligned} \right\} \dots \dots (12)$$

(b) When $(BG)^2 = 16kEI$,

$$\left. \begin{aligned} Y_1 + Y_2 &= (C_1 + C_2 x) e^{\nu_1 x} \\ &+ (C_3 + C_4 x) e^{\nu_2 x} \\ \nu_1 &= \sqrt{BG/(4EI)} \\ \nu_2 &= -\sqrt{BG/(4EI)} \end{aligned} \right\} \dots \dots (13)$$

(c) When $(BG)^2 < 16kEI$,

$$\left. \begin{aligned} Y_1 + Y_2 &= e^{\xi_1 x} (C_1 \cos \xi_2 x \\ &+ C_2 \sin \xi_2 x) + e^{-\xi_1 x} (C_3 \cos \xi_2 x \\ &+ C_4 \sin \xi_2 x) \\ \xi_1 &= \sqrt{(4\sqrt{kEI} + BG)/(8EI)} \\ \xi_2 &= \sqrt{(4\sqrt{kEI} - BG)/(8EI)} \end{aligned} \right\} \dots \dots (14)$$

From eq. (9),

$$\left. \begin{aligned} Y_1 - Y_2 &= e^{\alpha_1 x} (D_1 \cos \alpha_1 x \\ &+ D_2 \sin \alpha_1 x) + e^{-\alpha_1 x} (D_3 \cos \alpha_1 x \\ &+ D_4 \sin \alpha_1 x) \\ \alpha_1 &= \sqrt[4]{(2E_s + kB)/(4BEI)} \end{aligned} \right\} \dots \dots (15)$$

(2) Above ground ($x \geq 0$)

From eq. (10),

$$\left. \begin{aligned} y_1 + y_2 &= C_5 \cosh(\lambda x) \\ &+ C_6 \sinh(\lambda x) + C_7 x + C_8 \\ &- \frac{m}{3BG}(H - x)^3 - \frac{w}{BG}(H - x)^2 \\ \lambda &= \sqrt{BG/(2EI)} \end{aligned} \right\} \dots \dots (16)$$

From eq. (11),

$$\left. \begin{aligned} y_1 - y_2 &= e^{\alpha_2 x} (D_5 \cos \alpha_2 x \\ &+ D_6 \sin \alpha_2 x) + e^{-\alpha_2 x} (D_7 \cos \alpha_2 x \\ &+ D_8 \sin \alpha_2 x) \\ &+ \frac{mB}{2E_s}(H - x) + \frac{wB}{2E_s} \\ \alpha_2 &= \sqrt[4]{E_s/(2BEI)} \end{aligned} \right\} \dots \dots (17)$$

Sheet pile deflections on loaded and unloaded sides, and above and below the ground, y and Y , can be obtained immediately from $y_1 \pm y_2$ and $Y_1 \pm Y_2$ in eqs. (12)–(17) through the arithmetic calculation. Similarly, flexural angle, bending moment and shearing force of each sheet pile can be obtained by using derivatives.

2.2 Boundary Conditions of Double Sheet Pile Wall Structure

The top of this structure is often used as road through the concrete superstructure work¹⁴. The head constraining effects will be examined elsewhere, and the case of fastening two rows of sheet piles with tie rod alone will be considered here. It may be assumed that the tops of sheet piles are not subjected to the constraining moment of tie rods because tie rods are adequately compliant. However, the tension changes owing to the elastic deformation of tie rods caused by the relative deflection of two-rowed sheet piles. Additionally, it is assumed that the shear resistance of filling sand in proportion to the flexure angle of pile head acts equally to two rows of sheet piles.

At the ground surface, it is to be assumed that deflection, flexural angle, bending moment and shearing force for each of two-rowed sheet piles are continuous.

As the constraining force at the bottom of sheet pile below the ground is small, bending moment and shearing force may be regarded as zero.

On the basis of these assumptions, the following sixteen formulae for boundary conditions are obtained. At the top of sheet pile ($x = H$),

$$\left. \begin{aligned} y_1'' &= 0, & y_2'' &= 0 \\ y_1''' &= \frac{E_t A_t}{BEI}(y_1 - y_2) \\ &+ \frac{BG}{4EI}(y_1' + y_2') - \frac{P}{EI} \\ y_2''' &= -\frac{E_t A_t}{BEI}(y_1 - y_2) \\ &+ \frac{BG}{4EI}(y_1' + y_2') \end{aligned} \right\} \dots (18)$$

At the ground surface ($x = 0$),

$$\left. \begin{aligned} y_1 &= Y_1, & y_2 &= Y_2 \\ y_1' &= Y_1', & y_2' &= Y_2' \\ y_1'' &= Y_1'', & y_2'' &= Y_2'' \\ y_1''' &= Y_1''', & y_2''' &= Y_2''' \end{aligned} \right\} \dots (19)$$

At the bottom of sheet pile ($x = -D$),

$$\left. \begin{aligned} Y_1'' &= 0, & Y_2'' &= 0 \\ Y_1''' &= 0, & Y_2''' &= 0 \end{aligned} \right\} \dots (20)$$

- E_t : Young's modulus of tie rod
- A_t : Cross section of tie rod per unit width
- P : Concentrated load
- D : Penetration depth

When eqs. (18)–(20) are solved, unknown coefficients C_1 – C_8 and D_1 – D_8 can be obtained, allowing the prediction of the behavior of the structure.

3 Elasto-Plastic Calculation for Behavior of the Structure

According to the results of the previous experiments^{6,11)} as well as the present ones^{12,13)} by the authors, the deformational behavior of the double sheet pile wall structure is markedly non-linear from the earlier stage of external horizontal force. Since the sheet piles and tie rods behave elastically, it is evident that the non-linearity is attributable to the plasticity of filling sand and foundation ground. For this reason, while carrying out the experiment with small-¹²⁾ and large-sized¹³⁾ models of this structure, the authors conducted a simple shear test and a horizontal loading test for a row of sheet piles, in order to elucidate the shear modulus of filling sand and the coefficient of

horizontal subgrade reaction of penetrating segments in the plasticity domain. The present section concerns the mathematical expressions of these parameters and the method for elasto-plastic calculation of mechanical behaviors of this structure.

3.1 Estimation of Shear Modulus of Filling Sand

The grain size distributions of filling sand used for the small-¹²⁾ and large-sized¹³⁾ model experiments are shown in Fig. 3. The friction angle ϕ obtained from the triaxial compression test was 38.3° for the former, and 40.1° for the latter. The initial density γ_0 in the simple shear test was 1.52 – 1.53 (gf/cm³) for the former, and 1.62 – 1.65 (gf/cm³) for the latter, to be approximately equal to the weight of unit volume in the model experiments.

Figure 4 shows the relationship of secant shear modulus G to shear strain θ and normal stress σ_N , as derived from the simple shear test, with (a) for filling sand in the small-sized model experiment and (b) for that in the large-sized one. From this figure it may be concluded that the shear modulus G decreases approximately at a constant rate as θ increases for any value of normal stress $\sigma_N = 0.25, 0.50$ and 1.00 , and this relationship is estimated at $\theta^{-0.65}$ for (a) and $\theta^{-0.57}$ for (b).

Since the shear modulus grows also with the normal stress σ_N , an overall empirical relationship can be derived as follows by assuming that the upper limit of the horizontal head deflection/wall height ratio for this structure is 10^{-2} or so*, and the $G - \sigma_N$ relation can be approximated by a straight line at $\theta = 10^{-2}$ on the bilogarithmic plotting.

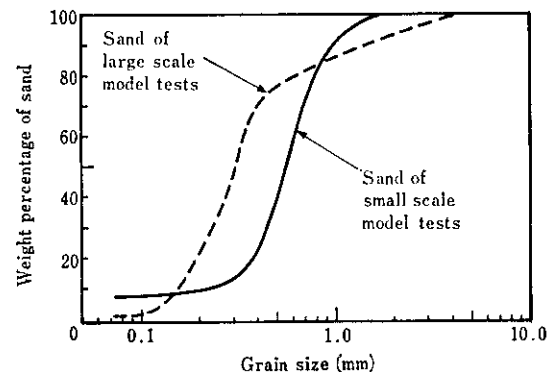


Fig. 3 Grain size distribution of filling sand used for model tests

Note: In the design¹⁾ of steel plate cellular cofferdams, the case where the horizontal deflection at the cell top is about 0.5% of the cell wall height is taken as the tolerable limit of deformation.

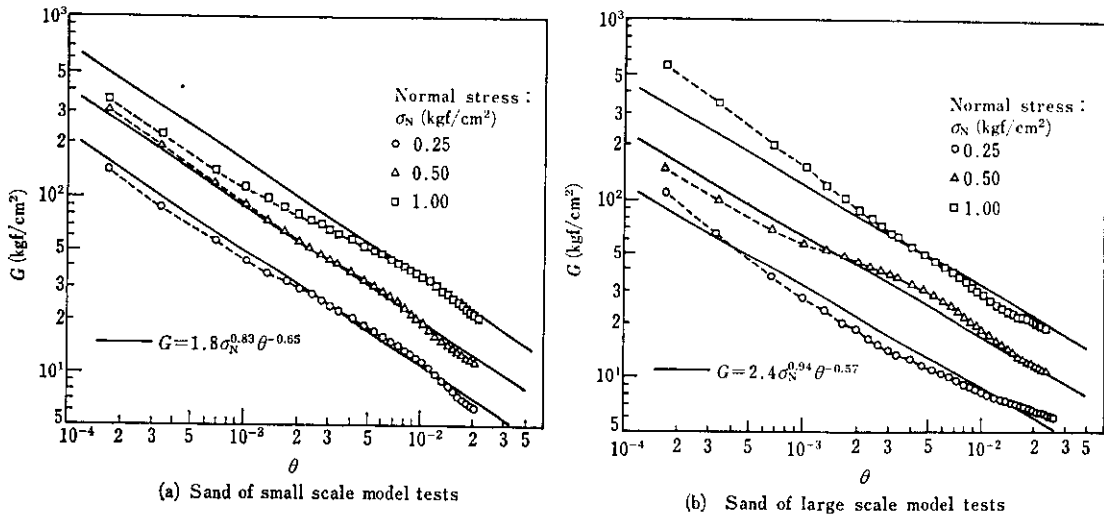


Fig. 4 Relation between shear modulus, G , and shear strain, θ , of filling sand

For filling sand used in the small-sized model experiment,

$$G = 1.8 \sigma_N^{0.83} \theta^{-0.65} \dots \dots \dots (21)$$

For filling sand used in the large-sized model experiment,

$$G = 2.4 \sigma_N^{0.94} \theta^{-0.57} \dots \dots \dots (22)$$

Solid lines in Fig. 4 represent the calculated values based on eqs. (21) and (22), and are supposed to indicate an overall trend of test values.

3.2 Estimation of Coefficient of Horizontal Subgrade Reaction

In order to obtain the coefficient of horizontal subgrade reaction k that corresponds to the penetrating segment of sheet pile, a horizontal load test¹⁵⁾ was conducted with a row of sheet piles. The height of the loading point above the ground surface is set to 9 cm and 50 cm in the small- and large-sized model experiments, respectively. The k -value was determined by putting measured values of load P and horizontal pile displacement at the ground surface y_g into Chang's formula for the horizontal behavior of single pile¹⁾.

Figure 5 shows the relationship of k to y_g and penetration depth D , with (a) and (b) for small- and

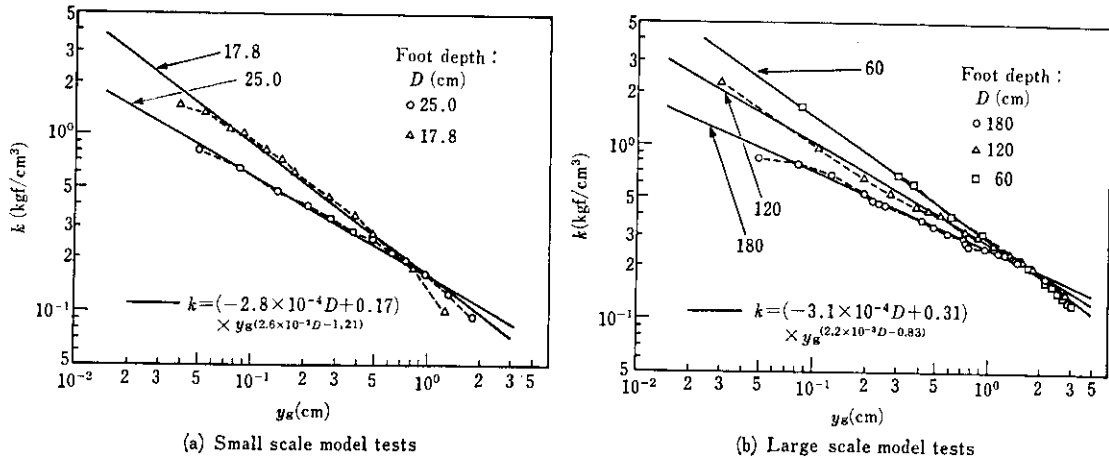


Fig. 5 Relation between coefficient of horizontal subgrade reaction, k , and displacement, y_g , of sheet pile at ground level

large-sized model experiments, respectively. It is evident that k decreases approximately at a constant rate as y_g increases, and the shorter the penetration depth D is, the steeper the slope becomes. Therefore, firstly, the slope was assumed to be represented as a linear function of D , with constants estimated as $(2.6 \times 10^{-2}D - 1.21)$ and $(2.2 \times 10^{-3}D - 0.83)$. Moreover, if the relationship of k to D at $y_g = 1.0$ cm is also assumed to be linear, the overall relationship may be approximated as below.

For the small-sized model,

$$k = (-2.8 \times 10^{-4}D + 0.17)y_g^{(2.6 \times 10^{-2}D - 1.21)} \dots (23)$$

For the large-sized model,

$$k = (-3.1 \times 10^{-4}D + 0.31)y_g^{(2.2 \times 10^{-3}D - 0.83)} \dots (24)$$

3.3 Method of Calculation

Since the theoretical solution does not take into consideration the distribution of shear modulus G , the elasto-plastic calculation with eqs. (21) or (22) was simplified by regarding normal stress σ_N and shear stress θ as constant, represented by certain tentative values. As for σ_N , the earth pressure by filling sand at a depth of $a(H + D)$ from the top of wall was taken as the representative value, as expressed by eq. (25), where a is a conversion factor to give the depth from the top of wall. The shear stress θ is given by eq. (26) in terms of horizontal deflection and wall height of the structure. (See Fig. 6.)

$$\sigma_N = a\gamma(H + D) \dots (25)$$

$$\theta = \left(\frac{y_{1t} + y_{2t}}{2} - \frac{y_{1g} + y_{2g}}{2} \right) / H \dots (26)$$

γ : Weight of filling sand per unit volume,

y_{1t}, y_{2t} : Horizontal deflections of tops of sheet piles, 1 and 2, respectively,

y_{1g}, y_{2g} : Horizontal deflection of sheet piles, 1 and 2, respectively, at the ground surface.

The Young's modulus of filling sand E_s is represented by the following equation with shear modulus G and Poisson's ratio ν :

$$E_s = 2(1 + \nu)G \dots (27)$$

In the calculation to be described in the following section, ν is set to 0.4 just like Hirashima et al.⁷⁾

In eqs. (23) and (24) for the coefficient of horizontal subgrade reaction k , y_g is calculated through the following formula:

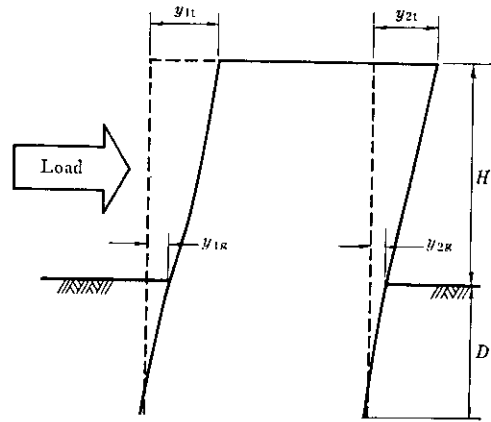


Fig. 6 Structure deformation

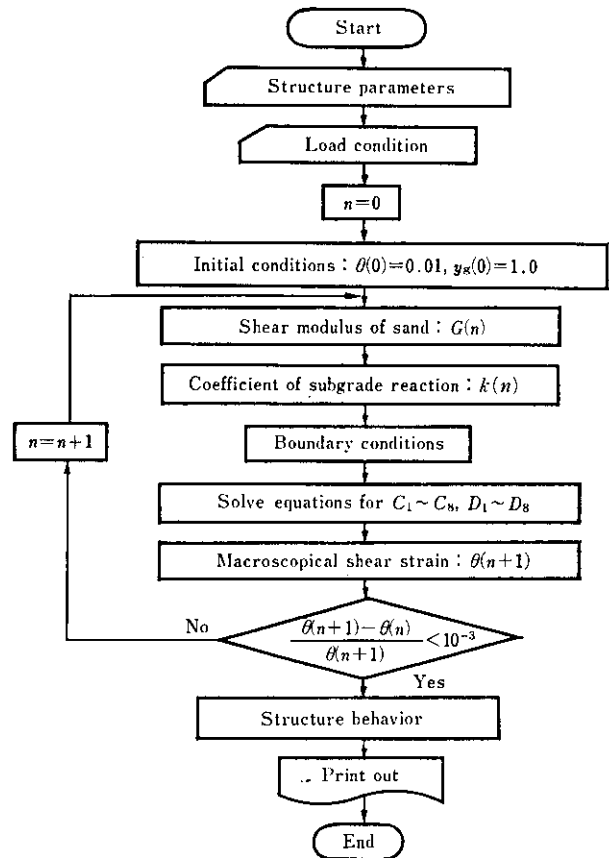


Fig. 7 Flowchart of elasto-plastic computation for double sheet pile wall structure

$$y_g = \frac{y_{1g} + y_{2g}}{2} \dots (28)$$

The iterative calculations with eqs. (12)–(28) permit the elasto-plastic analysis for the behavior of this structure. A flowchart for this analysis is shown in Fig. 7.

Table 1 Description of experiments

Model scale	Case No.	H (cm)	D (cm)	B (cm)	E ($\times 10^6$ kgf/cm ²)	I ($\times 10^{-2}$ cm ⁴ /cm)	E _t ($\times 10^6$ kgf/cm ²)	A _t ($\times 10^{-2}$ cm ² /cm)	γ (gf/cm ³)	ρ (cm ² kgf ⁻¹ /cm)	Number of loading point
Small	1	71.4	17.8	50.0	0.686	0.256	0.296	0.392	1.58	14 800	4
	2	50.0	17.8	50.0	0.686	0.268	0.296	0.392	1.51	3 400	4
	3	38.5	17.8	50.0	0.686	0.279	0.296	0.392	1.54	1 150	3
Large	4	160.0	117.0	170.0	2.1	158.0	2.1	5.7	1.62	198	3
	5	160.0	60.0	170.0	2.1	159.0	2.1	5.7	1.62	196	3
	6	160.0	117.0	170.0	2.1	158.0	2.1	5.7	1.62	198	1

H : Wall height
 D : Penetration depth
 B : Wall breadth
 E : Young's modulus of sheet pile
 I : Geometrical moment of inertia
 E_t : Young's modulus of tie rod
 A_t : Cross section of tie rod
 γ : Unit weight of filling sand
 ρ : Flexibility number ($= \frac{H^4}{EI}$)¹⁶⁾

4 Comparison of Calculated Values with Experiment

Details of the model experiment are reported elsewhere^{12,13)}. Parameters for the experimental cases to be compared with calculated values in this section are listed in Table 1. Nos. 1-5 are for cases of loading at plural points with distributed load assumed, and No. 6 for cases with load concentrated at the top of sheet pile.

Figure 8 shows the relationship of horizontal deflection y_{2t} , of sheet pile top on the unloaded side to total load, indicating that the calculated values conform well to the elasto-plastic behavior of the experimental values. The conversion factor a for the normal stress of filling sand is selected so that the calculated value corresponds with the experimental value when y_{2t} is about 1% of wall height.

For the small-sized model (a), the smaller the wall height H , the greater the a -value becomes. On the

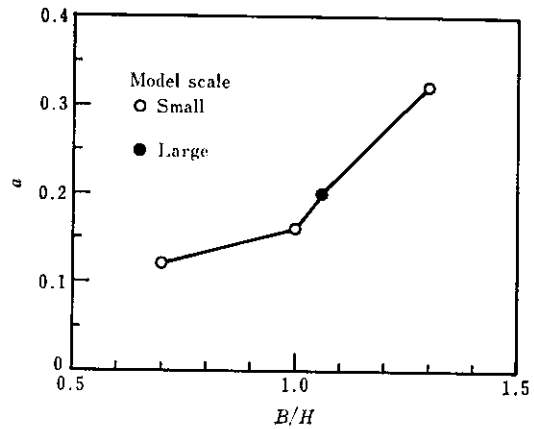


Fig. 9 Relation between modulus, a , for normal stress of filling sand and relative breadth, B/H , of wall

other hand, with the large-sized model (b), calculated values with $a = 0.2$ for cases with different penetration lengths and load conditions correspond with experimental values. Figure 9 shows the relationship

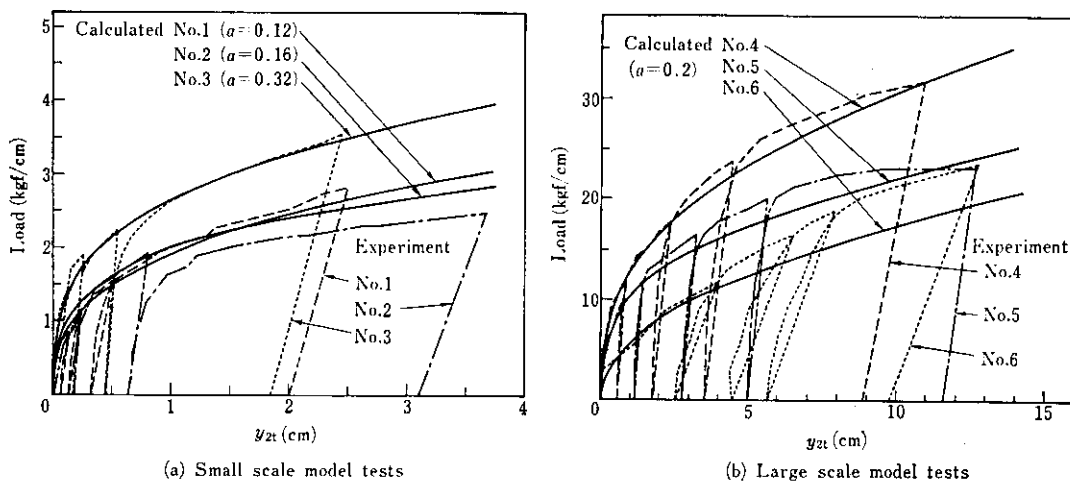


Fig. 8 Comparison between calculated curves and experimental data for horizontal displacement of wall top

of a to the breadth-to-height ratio B/H of the wall. For both small- and large-sized models, a tends to grow as the B/H ratio increases. In the subsequent calculation, a -value given in Fig. 9 is adopted.

The distribution of bending moment in sheet pile is shown in Fig. 10 (a)–(e), of which (a)–(c) concern the comparison under the loading conditions based on the distributed load for the small-sized model. The calculated value well represents changes in the distribution pattern of moment between two-rowed sheet piles in respect to wall height. The negative bending moment occurring above the ground is attributable to shear resistance of filling sand. Here, both calculated and experimental values present similar trends, suggesting the appropriateness of the calculation model including the interaction between sheet piles and filling sand. On the other hand, (d) represents the case of loading with the large-sized model under the sim-

ilar conditions as in (a)–(c). The experimental value of negative bending moment at the sheet pile above the ground on the loaded side is much smaller than the calculated value. In case of large-sized model, the shear resistance supposedly fails to manifest itself fully because filling sand at the top of sheet pile on the loaded side succumbs to the pressure from sheet pile and results in plastic collapse because the flexural rigidity of sheet pile is large in comparison with the wall height of model, as is evident from the fact that the flexibility number, ρ , of sheet pile defined by Rowe¹⁶⁾ is as small as 2×10^2 , as shown in Table 1. Since the flexibility number ρ is in the order of 10^3 ($\text{cm}^2 \cdot \text{kgf}^{-1} / \text{cm}$) in the sheet pile structural in general¹⁷⁾, close to that of small-sized model, the present calculation seems to provide a relatively good prediction for the distribution of bending moment in sheet pile under the distributed load. The case of loading at

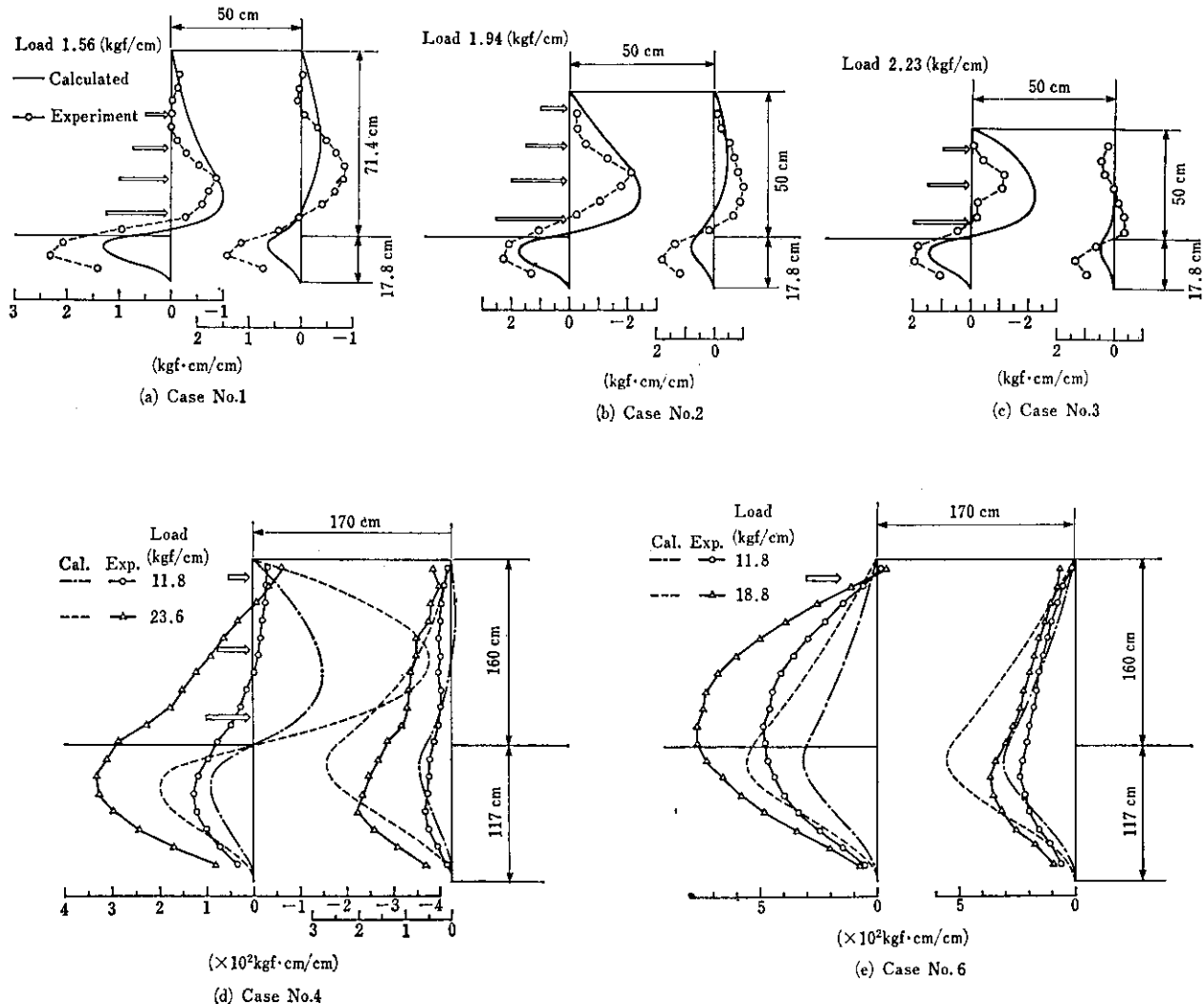


Fig. 10 Comparison between calculated curves and experimental data for bending moment distribution

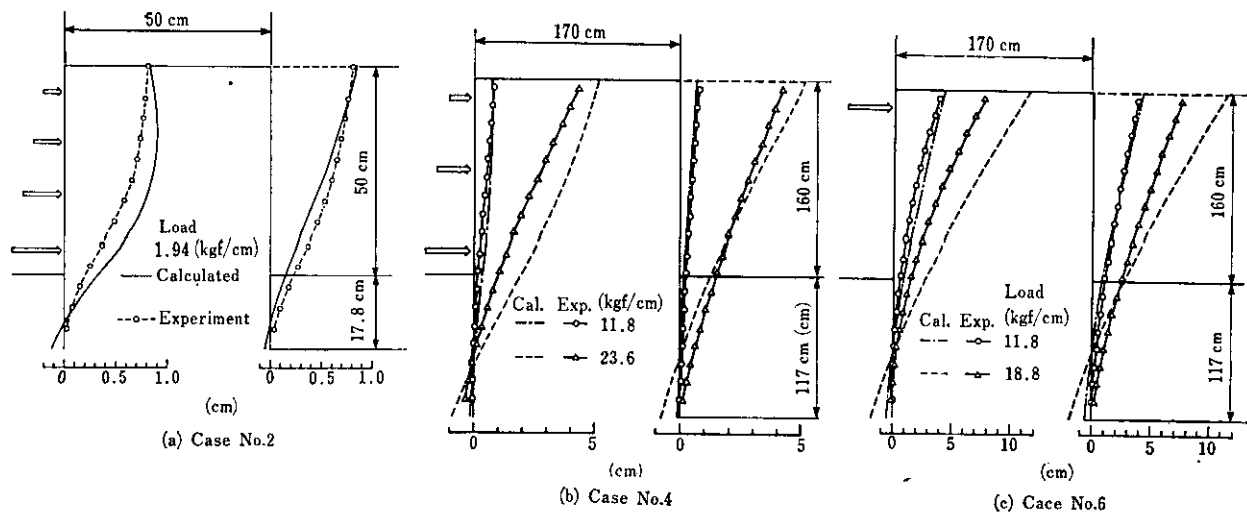


Fig. 11 Comparison between calculated curves and experimental data for horizontal displacement distribution

the top of sheet pile is shown in (e), where the calculated value fails to reflect the experimental result whereby the bending moment of sheet pile on the loaded side is greater than that on the unloaded side. This may be attributed to the discrepancy that the present calculation model assumes the transmission of stress through horizontal deformation only, while filling sand forms circular sliding surface¹²⁾ centered at the penetrating segment of sheet pile on the loaded side in case of loading concentrated at the top, requiring the consideration of the normal component of deformation in the vertical direction.

The distribution of horizontal deflection in sheet pile is shown in Fig. 11 (a)–(c). In (a), the calculated value represents well the behavior of shear deformation of the model wall. The experimental values shown in (b) and (c) indicate that the sheet pile on the loaded side rotates around the middle of penetrating segment, while that on the unloaded side around the bottom of penetrating segment, with sheet pile spacing expanded in the vicinity of ground surface. This may be due to the fact that filling sand sinks along the main sliding surface with the deformation of wall and presses the sheet piles on the unloaded side. The present calculation model fails to predict such a behavior.

5 Conclusions

In order to elucidate the mechanical characteristics of the double sheet pile wall structure under external horizontal force, the elasto-plastic analysis was carried out to compare with the experimental values, and the following conclusions were derived.

- (1) As for the horizontal deflection of sheet pile top, the calculated values well corresponded with the

experimental values. The conversion factor was $a = 0.12-0.32$ for the breadth-to-wall height ratio $B/H = 0.7-1.3$ and tended to grow with B/H .

- (2) When the flexibility number, ρ , of sheet pile was adequately large and the external force was a distributed load, the calculated value for the distribution of bending moment in sheet pile corresponds relatively well with the experimental values.
- (3) When the flexibility number, ρ , of sheet pile was small and the rigidity of sheet pile is large in comparison with the wall height, or when the normal component of deformation of filling sand predominates as in case of large-sized model, the calculated values failed to correspond with the experimental ones with respect to the distribution of bending moment and deflection. In the present analysis, the normal distribution of shear modulus of filling sand and the effects of sliding surface formation and local plastic collapse in filling sand are not taken into account for the sake of simplicity. In the large-sized model, on the other hand, light-weight steel sheet piles which had the least flexural rigidity among the currently available sheet piles so as to grasp the behavior of sheet pile joint. Since these piles presented relatively little flexure in the model experiment, it was supposed that the effects of sliding or localized plastic collapse in filling sand were exaggerated. As the failure of correspondence between the calculated and experimental values is attributable to these factors, it seems necessary to examine in further detail.

To sum up, with regard to the deformation of wall and the bending moment of sheet pile which constitute

the most important design data, the calculated values agree well with the experimental values as long as the flexure of sheet pile, one of general characteristics of actual double sheet pile wall structure, is large. This may be regarded to suggest the practical applicability of the present theoretical treatment. On the other hand, however, the discrepancy between the calculation model with the equilibrium between horizontal forces alone taken into consideration and the structural characteristics of experimental model was made clear. Regrettably, the head-constraining effects of superstructure concrete and the effects of normal stress distribution in filling sand were not examined at all. It is being attempted to improve the present calculation model for the better predictive accuracy of mechanical behavior, and to incorporate new calculation methods and factors so as to pursue the study toward the application to a synthetic design.

References

- 1) Japan Harbor Association: Technical Standards for Harbor Facilities, (1979) Japan Harbor Association
- 2) Cummings, E. M.: Cellular Cofferdams and Docks, Harbours Div., ASCE, WW3, (1957) Paper 1366, pp. 1-29
- 3) S. Kitajima: "Study on the stability of cellular bulkheads" *Monthly Reports of Transportation, Technical Research Institute Ministry of Transportation*, 12(1962) 3, pp. 1-101
- 4) Mazurkiewicz, B.: A solution to the stability problem of the double sheet wall cofferdam, based on Brinch Hansen's Earth Pressure Theory, *Arch. Hydrot.*, XV(1968) 3, pp. 429-472
- 5) M. Sawaguchi: "A calculation method of a double-wall cofferdam", *Technical Note of the Port and Harbour Research Institute Ministry of Transportation*, (1972) 132, pp. 3-13
- 6) M. Sawaguchi: "Lateral behavior of a double sheet pile wall structure", *Journal of the Japanese Society of Soil Mech. and Found. Erg.* 14(1974) 1, pp. 45-59
- 7) T. Hirajima, K. Aoki, and K. Okamoto: "Analysis of double sheet pile wall structure through the finite element method", 29th Annual Congress of Civil Engr. Society, III-128, (1974)
- 8) N. K. Burki, et al.: "Photoelastic analysis of a cofferdam", *J. Geotechnical Div. ASCE*, GT2(1975), pp. 129-145
- 9) C. Takahashi, M. Ishida, and H. Miyoshi: "Experimental study on vibrational properties of double sheet-piled wall structure", *Kawasaki Steel Technical Report*, 7(1975) 3, pp. 60-76 (in Japanese)
- 10) H. Arai, C. Takahashi, and M. Ishida: "On the vibration characteristics of double sheet pile wall structure", *The Japanese Society of Soil Mechanics and Foundation Engineering*, 24(1976) 5, pp. 55-61
- 11) M. Sawaguchi, F. Shima, and H. Miyoshi: "Static behavior of double sheet pile revetment", *ibid. The Japanese Society of Soil Mechanics and Foundation Engineering*, 24(1976) 4, pp. 19-26
- 12) T. Yagyu, et al.: "Model test of the double sheet pile wall structure", 17th Conference on Soil Mechanics and Foundation Erg. H-2, (1982), pp. 729-732
- 13) K. Ohori, et al.: "Large-scale model test of double sheet pile wall structure", 18th Conference on Soil Mechanics and Foundation Erg.: H-7, (1983) pp. 1 147-1 150
- 14) T. Shimizu, et al.: "Construction of closing dike with double piling and some measurement under works", *Kumagai Giho* (1980) 27, pp. 89-105
- 15) K. Ohori et al.: "Coefficient of horizontal subgrade reaction for a row of sheet piles" 38th Annual Congress of Civil Engr. Society III-307 (1983)
- 16) P. W. Rowe: "A theoretical and experimental analysis of sheet-pile walls", *Proc. Instn. Civ. Engrs.*, Pt.I (1955) 4
- 17) K. Ishiguro, M. Shiraishi and H. Kaiwa: "Sheet Pile Works", Part I, (1982), p. 150, Sankai-Do